

## A NEW ANALYSIS OF THE SEASAT TRACKING DATA

L G Agrotis & J M Dow

European Space Operations Centre (ESOC),  
Robert-Bosch-Str. 5, 6100 Darmstadt, FRG  
\* LOGICA SDS Ltd.

### ABSTRACT

SEASAT orbit determination is being used as one of several tools for validating the ESOC orbit determination software in preparation for the ERS-1 mission. The paper discusses the results of a new analysis of the SEASAT laser and S-band tracking data, using models that have been developed in the last few years. A new laser station set has been derived from the tracking data, while new S-band station coordinates have been obtained from combination solutions. These station solutions are compared with those from earlier analyses. The accuracy of the determined SEASAT orbits is assessed by comparing the S-band and laser solutions. The results of SEASAT orbit determination are also compared with those obtained from ERS-1 simulations and with ERS-1 accuracy requirements.

Keywords: SEASAT, satellite altimetry, orbit determination, geodesy, laser ranging, ERS-1, remote sensing.

### 1. INTRODUCTION

SEASAT is a remote-sensing satellite launched by NASA in June 1978. Although it failed after only 106 days in orbit, it provided a wealth of scientific data which are still being analysed. The main reason for processing SEASAT data at ESOC lies in the great similarities between it and ERS-1, which is due for launch by ESA in 1990. Both satellites carry a synthetic aperture radar, a radar altimeter, and a wind scatterometer as part of their payload. More importantly, both fly in similar orbits and are tracked by similar types of measurements and tracking networks. A set of SEASAT and ERS-1 mean orbital elements are given in Table 1.

DESCRIPTION	UNITS	SEASAT	ERS-1
Nodal Period	min	100.8	100.5
Semi-Major Axis	km	7172.3	7153.1
Inclination	deg	108.0	98.5
Eccentricity	-	0.0008	0.0011
Altitude	km	797	778

Table 1: SEASAT and ERS-1 Mean Elements  
(3-Day Repeat Orbits)

SEASAT was tracked by three independent station networks:

- o An S-band doppler network comprising approximately 16 stations with a good geographic distribution, for the operational tracking.
- o A laser network of around 10 stations, mainly in North and South America.
- o The US Navy TRANET network consisting of over 40 widely distributed sites.

The laser network was used for precise orbit determination and for the in-flight calibration of the radar altimeter. The data from the TRANET network, which had the best coverage, has not yet been released. The tracking data available at ESOC consists therefore of the laser ranges and of the S-band doppler measurements. The objectives of the work outlined in this paper are to test ESOC orbit determination capabilities in preparation for the ERS-1 mission and to investigate the achievable ERS-1 orbit accuracies, by analysing the SEASAT data and interpreting the results as being applicable to ERS-1.

The SEASAT data were processed with the ESOC orbit determination program, BAHN, which has recently been upgraded to include the most up-to-date dynamical and measurement models available (see Refs. 3 and 5). The important components of these models, used in the analysis of the SEASAT data, are outlined in Table 2.

DESCRIPTION	MODEL
Earth gravity	PGS-64 (36 x 36)
Air drag	MSIS 77 - Adjusted drag coefficient
Direct solar radiation	Adjusted radiation pressure coefficient
Moon and Sun attraction	DE200/LE200 ephemeris
Solid Earth tides	$k_2=0.3, h_2=0.6, l_2=0.075$
Ocean tides	Schwiderski model
Precession	IAU 1976
Nutation	IAU 1980
Sidereal time	New relationship between GMST and UT1
Coordinate system	Mean equator and equinox of 2000.0 (J2000)
UT1	BIH values
Pole	BIH for laser station estimation runs, otherwise estimated from data

Table 2: SEASAT Dynamic and Measurement Models



2. ANALYSIS OF SEASAT LASER RANGE OBSERVATIONS

The laser stations at the time of SEASAT launch had accuracies of 10-50 cm. The main drawbacks of this network are the non-optimal coverage, with most stations being located in middle and low latitude areas of North and South America, and the fact that only a fraction of the SEASAT passes were tracked (lasers cannot observe through clouds). For these reasons it was decided to process limited sets of data with relatively good coverage. Seven 3-day arcs were selected (see Ref. 1) and analysed separately. The stations contributing data to these arcs are shown in Figure 1. It can be seen that only Kootwijk (Netherlands) provided data from Europe. However, it contributed data to only one of the selected arcs and its contribution was therefore not significant.

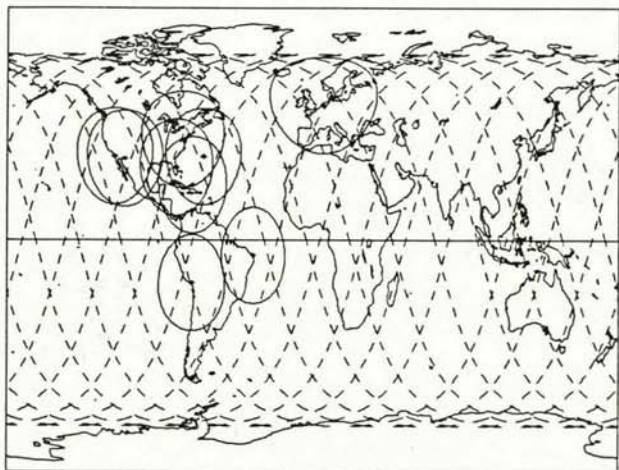


Figure 1. Seasat 14-revolution arc and coverage circles for selected laser network

After some initial tests with the laser data it was realised that the PGS-S4 coordinates were not compatible with the new models used in BAHN. It was decided to attempt to derive new station coordinates from the seven 3-day arcs. The results from these estimations are summarised in Table 3. Because of the high drag values observed in arc 7 its contribution to the derivation of the final station coordinates was excluded. To avoid using excessive amounts of data from stations with high laser pulse rates, the minimum time allowed between successive observations was 5 seconds. No attempt was made to derive normal points, but a coarse rejection criterion was adopted to eliminate bad observations.

The solutions outlined above resulted in the derivation of 6 sets of station coordinates. These sets were derived using the BIH values for the pole and for UT1. In order to remove any residual pole and UT1 errors a 3-rotation transformation was applied to each of 5 sets, so that their individual reference axes were aligned as much as possible to the reference frame of the station solution from arc 5. The final coordinates of the laser stations were the mean

values of the 6 sets, after the 3-rotation transformations. In Table 4 we assess the internal and external consistency of the final station solution. The RMS standard deviations about the mean values were under 2 m in each component. The table also shows the RMS standard deviations about the mean values when the mean coordinates were evaluated without the 3-rotation transformations. The discrepancies in latitude were considerably larger, at about 4 m, reflecting the effect of residual pole errors. The RMS differences between the PGS-S4 and ESOC solutions were at the 2.5 m level for longitude and latitude, and at the 4 m level for height. When a 3-rotation transformation was applied to the PGS-S4 coordinates, these differences reduced to 0.6 m in longitude, 1.4 m in latitude and 3.8 m in height, signifying that they were largely attributable to pole errors. The height discrepancies arose because of significant (7 m) differences for the heights of the two SAO lasers at Arequipa (Peru) and Mt. Hopkins (Arizona). When these stations were ignored, the rms height differences reduced to 0.7 m.

In order to assess the improvement realised with the new station coordinates the orbit determinations were repeated twice. For the first case the ESOC-derived coordinates were held fixed in each arc, in determinations for the SEASAT orbit, a drag and radiation pressure coefficient, and the coordinates of the pole. For the second case the same determinations were performed, but this time the PGS-S4 coordinates were held fixed. Figure 2 is a plot of the RMS residuals for each arc. It can be seen that an improvement of approximately 1 m in the residuals has been achieved when using the new stations coordinates.

Arc ID	Epoch (0 hrs dd mm)	No. of stat. estim.	No. of passes	No. of laser ranges	C <sub>d</sub>	C <sub>r</sub>	rms resid (m)
1	08 08	5	21	672	0.72	1.12	1.30
2	11 08	4	10	359	1.18	1.03	0.58
3	14 09	7	18	646	1.03	1.35	0.91
4	19 09	7	27	878	0.91	1.13	1.10
5	22 09	7	27	774	2.10	1.63	0.83
6	25 09	7	22	761	2.95	0.67	1.25
7*	28 09	6	15	665	4.26	2.73	1.41

\* Not used in derivation of station coordinates

Table 3. Results of laser station estimation runs

Station	No. of arcs used	Standard Deviation			PGS-S4 - ESOC		
		long.	lat.	ht.	long.	lat.	ht.
ARELAS 9907	6	0.6	1.1	1.6	0.0	-0.4	-7.9
SANO76 7062	5	1.7	0.8	1.0	1.7	2.3	-0.5
RAMIAS 7069	6	0.5	1.3	1.6	3.0	1.2	0.8
SIALIAS 7063	2	1.5	0.4	1.0	3.4	2.5	-0.8
HOPLAS 9921	3	1.1	0.5	3.0	1.5	4.3	-6.2
GRILAS 7068	4	1.1	1.7	2.3	2.4	-2.3	-0.6
BDALAS 7067	5	1.1	1.3	1.2	2.3	-2.1	0.7
RMS		1.2	1.2	1.8	2.3	2.4	3.8
RMS before 3-rot.		1.7	3.7	1.8	2.2	3.0	3.8

Table 4. Evaluation of SEASAT laser station solutions



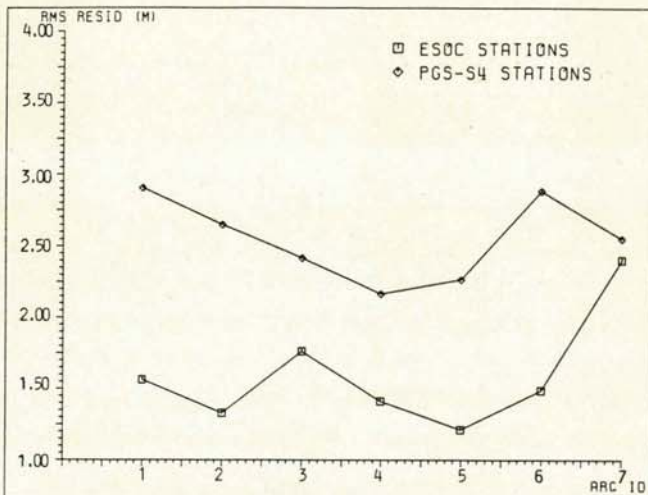


Figure 2. RMS residuals from SEASAT laser solutions. Station coordinates held fixed. Orbit, drag, radiation pressure and pole estimated.

### 3. ANALYSIS OF S-BAND DOPPLER DATA

The SEASAT S-band data consisted of Doppler range-rates integrated over intervals of typically 30 seconds. In the ESOC software these data were treated as range differences by multiplying the range-rates by the given integration intervals. For the S-band analysis it was decided to use the same 3-day arcs of data as for the laser solutions, in order to enable comparisons between them. The 10 degree elevation circles for the S-band stations that contributed observations during these 3-day arcs are shown in Figure 3. It is seen that the S-band network had a much more favourable coverage than the laser network. The station in Alaska was in a position to receive 7-8 passes per day, and in fact it contributed most of the observations.

The main problem with the S-band data was the fact that they were observed on only one frequency, requiring a model to remove the errors arising from ionospheric delays. A simple model was used, where these delays were assumed to be inversely proportional to the sine of the satellite elevation. An ionospheric scaling parameter per station, corresponding to the value of the ionospheric range error at zenith, was estimated for each 3-day arc. The magnitude of this parameter was found to be approximately 3 m. A drawback of this approach is that it assumes that the ionospheric scaling parameter at each station remains constant for all passes during a 3-day arc. Nevertheless, as will be seen in the next section, the above model gave satisfactory results. It is planned to investigate the effect of including more complex models, as for example the one due to Bent/Rawer (Ref. 10) which is available at ESOC.

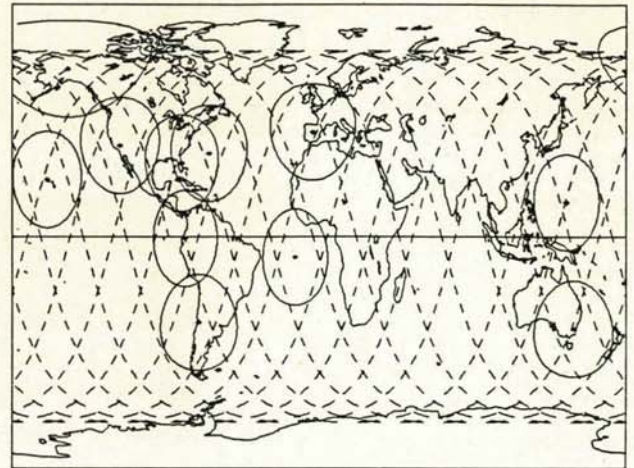


Figure 3. SEASAT 14-revolution arc and coverage circles for selected S-band network

### 4. COMPARISONS BETWEEN LASER AND S-BAND DETERMINATIONS

A number of determinations were performed in order to compare the results given by the laser and the S-band networks. In these determinations the force and measurement models outlined in Table 2 were used. The ESOC derived station coordinates were used for the laser solutions, while the PGS-S4 coordinates were used for the S-band. For both types of data the estimated parameters in each 3-day arc were the SEASAT orbital elements, a drag coefficient, a radiation pressure coefficient and the coordinates of the pole. In addition, as explained in the previous section, an ionospheric scaling parameter per station was estimated in the S-band solutions.

Figure 4 shows the laser and S-band solutions for the drag coefficient  $C_D$  in each arc. There is extremely good agreement between the two networks, and in both cases there is a sharp increase of the  $C_D$  values in arcs 6 and 7. This increase can be correlated to the level of geomagnetic activity at the time (see Figure 5). It appears that the available drag models (MSIS 77 in this case, but also other models gave similar results) cannot cope adequately with periods of intense geomagnetic activity. A perfect model would give constant values of  $C_D$  over all arcs, provided changes in the spacecraft cross-sectional area with respect to the atmosphere were modelled perfectly. These changes were not modelled in our software but this does not explain the observed variations in  $C_D$ . In addition, estimation of daily  $C_D$  values (instead of the 3-day values estimated in these determinations) would have resulted in better fits to the data.

Figure 6 shows the RMS SEASAT orbit differences between the laser and S-band solutions, resolved in the orbital reference frame. These differences are measures of the absolute orbit error, since the two networks are entirely independent. If one overlooks the results from arc 7 (extremely high drag, insufficient laser coverage) it appears that the RMS radial orbit error is of the order of 1 m. Even better accuracies should be achievable for ERS-1 when it is tracked by a number of PRARE



and laser stations. Simulations at ESOC (Ref. 2) and at Delft University (Refs. 11 and 12) indicate that 10-20 cm RMS radial orbit accuracies are feasible, after elimination of the gravity field errors by evaluating a tailored ERS-1 gravity model. Such accuracies are required in order to support the ERS-1 altimetry mission. Figure 6 also shows that the SEASAT along-track errors are of the order of 6-8 m, while the cross-track errors are at the 1-3 m level.

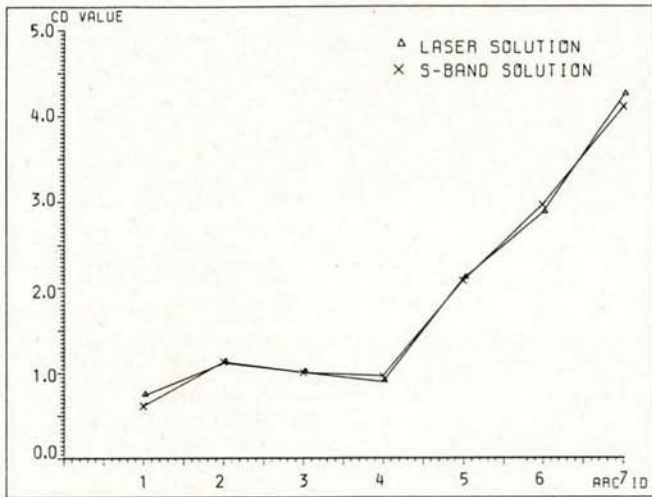


Figure 4. Comparison of drag coefficient estimation

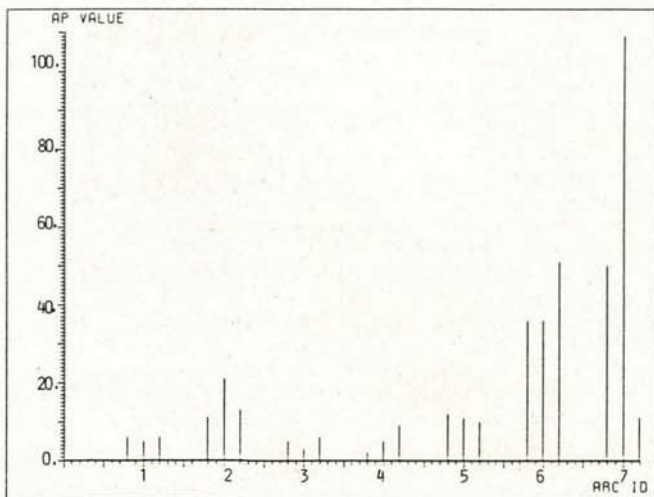


Figure 5. Daily geomagnetic index ( $A_p$ ) during SEASAT arcs

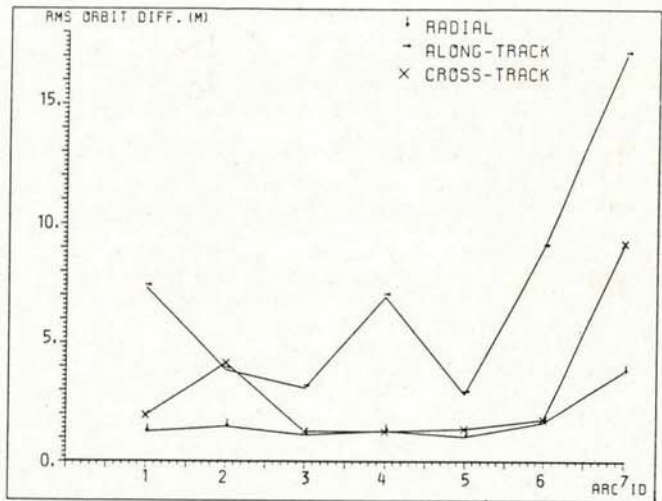


Figure 6. RMS orbit differences between laser and S-band

Figure 7 is a plot of the differences between the BIH and the ESOC xp pole solutions. It can be seen that there is a bias of about 0.15 asec between the laser and S-band solutions, indicating a difference between the laser and the S-band station reference frames. The laser solution appears to be the noisiest of the two, giving results that are clearly erroneous for arc 7. This is due to the high drag and to the insufficient laser tracking coverage for this arc.

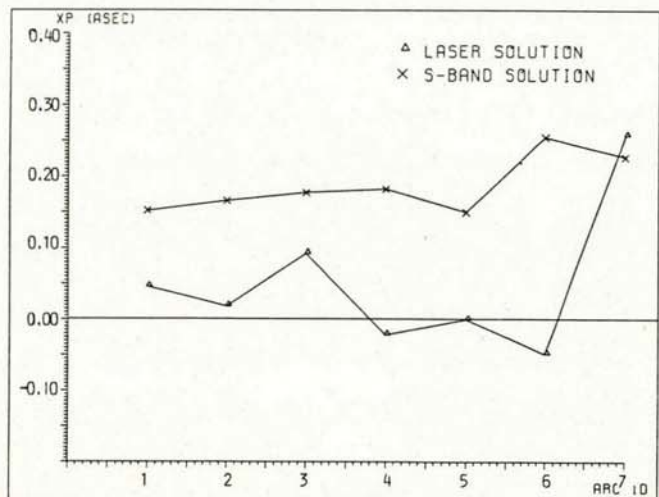


Figure 7. Comparison of xp pole estimation (ESOC-BIH)

5. COMBINATION LASER AND S-BAND SOLUTIONS

Combination solutions are of interest for support of the SEASAT and ERS-1 altimetry missions, because they provide a means of increasing the coverage by utilising all the available data. They are also valuable for estimating all station coordinates on a single reference frame. The first problem when dealing with combinations of



more than one type of tracking measurement is the choice of weights to assign to each type. For the preliminary analysis performed at ESOC the laser ranges were given a standard error of 1 m and the range-differences 50 cm (corresponding to 1.7 cm/s for range-rate). The same seven 3-day arcs of data as before (see Table 2) were used in determinations of the SEASAT orbit, drag, radiation pressure, pole coordinates, the coordinates of the S-band stations, and one ionospheric scaling parameter per S-band station. The laser station coordinates were held fixed at the ESOC-determined values. The results from the combination solutions were very close to those from the laser-only solutions. This implies that the weighting chosen gave most importance to the laser data. More tests, especially comparisons with the altimetry, are required in order to assess whether any improvements can be realised by changing the relative weighting between laser and S-band.

The most important result of the combination solutions was the estimation of the S-band station coordinates. An assessment of these is given in Table 5. The standard deviations of the station coordinates about their mean values were at the 3-5 m level. This was also the level of agreement between the mean coordinates from the first 6 combination arcs and the PGS-S4 station set. In the latter case the heights gave better agreement than the values for longitude and latitude, signifying different reference frame definitions between the ESOC-derived laser station coordinates and the PGS-S4 S-band stations. This result can also be confirmed by referring again to Figure 7, where the xp pole solutions show a 0.15 asec (4.5 m) bias between laser (ESOC stations) and S-band (PGS-S4 stations) pole estimates. A 3-rotation transformation of the PGS-S4 coordinates reduced the differences in longitude and latitude to 2.9 m and 0.8 m respectively.

Station	No of arcs used	Standard Deviation			PGS-S4 - ESOC (m)			
		long.	lat.	ht.	long.	lat.	ht.	
Alaska	18	6	1.8	2.0	1.1	2.7	4.2	-1.5
Hawaii	12	6	3.9	2.2	4.0	1.5	5.7	-1.7
Goldst.	16	4	3.8	2.6	2.8	2.2	3.1	-1.8
Madrid	23	5	1.2	2.8	0.9	3.3	-5.3	-2.1
Guam	24	6	1.8	4.8	1.3	-3.8	5.6	-0.4
Goldst.	28	3	9.4	3.6	2.9	9.7	1.4	1.2
Florida	40	5	2.2	1.1	4.1	2.4	0.2	-2.4
Chile	54	5	8.3	4.3	5.1	1.9	2.7	-3.3
Florida	71	5	3.0	1.2	1.4	4.1	0.1	-2.2
RMS			4.6	3.0	3.0	4.2	3.8	2.0

Table 5. Evaluation of SEASAT S-band station solutions

## 6. ASSESSMENT OF ERS-1 OPERATIONAL ORBIT DETERMINATION ACCURACY

ERS-1 will be tracked, for operational purposes, by S-band ranging and Doppler from Kiruna (Sweden), with Villafranca (Spain) as back-up (see Figure 8). Work performed at ESOC in evaluating the ERS-1 operational orbit determination and prediction accuracies using the SEASAT laser data has already been reported in Ref. 1. The recent analysis of the S-band data provided a possibility to use the high latitude SEASAT station in Alaska in order to simulate Kiruna tracking of ERS-1.

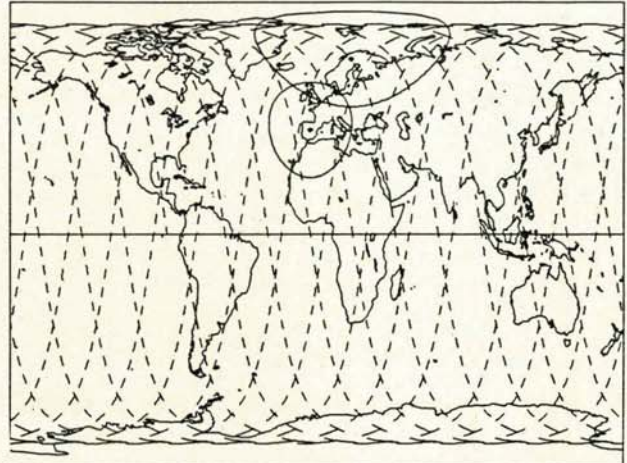


Figure 8. ERS-1 14-revolution arc with Kiruna and Villafranca visibility circles

The orbits determined with Alaska-only Doppler data, for arcs 1-6, were compared with the laser solutions. The assumption is that the differences are a measure of the Alaska orbit determination errors. In the laser solutions the station coordinates were held fixed at their ESOC-derived values. In the S-band solutions the coordinates of Alaska were held fixed at the PGS-S4 values. The estimated parameters in each arc, common to both laser and S-band, were the SEASAT orbit, and a drag and radiation pressure coefficient. In addition, pole coordinates were estimated from the laser data, while the S-band solutions estimated one ionospheric scaling parameter for Alaska. The RMS and maximum SEASAT orbit differences for each arc between the Alaska and the S-band solutions are given in Table 6. These are compared with the results of ERS-1 error analysis (see Refs. 1 and 2) and with operational orbit accuracy requirements for ERS-1. There is close agreement between the RMS values of the SEASAT orbit differences and the simulation results for ERS-1. Only the SEASAT values for arc 6 exhibit significantly larger orbit differences than the ERS-1 simulation errors, probably due to the higher drag observed in this arc. Both the ERS-1 simulation and the tests with the SEASAT data show that ERS-1 operational orbit determination requirements can be satisfied.



Arc ID	Radial		Along		Cross	
	Max	RMS	Max	RMS	Max	RMS
1	4.3	3.0	27.4	16.7	7.9	5.5
2	2.2	1.4	10.1	8.0	11.3	8.3
3	4.8	3.3	11.8	8.6	2.3	1.6
4	6.6	4.0	16.1	11.2	11.2	8.0
5	4.0	2.9	10.5	5.9	8.0	5.7
6	13.8	8.5	40.7	25.9	2.0	1.5
All Arcs	13.8	4.5	40.7	14.4	11.3	5.8
ERS-1 Simulation	8.7	5.8	26.4	14.1	6.7	4.6
ERS-1 Requirement	25		60		15	

SEASAT orbit differences between Alaska S-band tracking and the full laser network solutions. ERS-1 Kiruna S-band ranging simulation. Units in m.

Table 6. Evaluation of 1-station orbit determination accuracy

#### 8. CONCLUSIONS

1. The analysis of SEASAT data is an essential exercise in preparation for the ERS-1 mission.
2. SEASAT laser station coordinates with accuracies of better than 2 m have been derived from limited amounts of data.
3. Comparisons between SEASAT S-band and laser determinations indicate that achievable radial orbit accuracies are at the level of 1 m. These could be further improved for ERS-1 with better tracking coverage and air drag modelling. Also, the current laser stations are nearly one order of magnitude more accurate than the ones available at the time of SEASAT.
4. Combination SEASAT laser and S-band solutions resulted in the determination of the S-band station coordinates with accuracies of better than 5 m. A limiting factor was the modelling of the ionospheric errors in the S-band data.
5. Tests with SEASAT data have verified Kiruna capabilities to satisfy ERS-1 operational orbit accuracy requirements.

#### 9. REFERENCES

1. Agrotis L G, Dow J M and Lecohier G 1985, Orbit determination for altimetry missions, Pres. 26th Plenary Meeting of COSPAR, Symposium on Precise Orbit Computation, Toulouse, July 1986.
2. OAD-WP-284 (ESOC) 1985, Orbit determination of ERS-1 using S-band ranging and Doppler, laser ranging, PRARE and altimeter data, by Dow J M.
3. OAD-WP-293 (ESOC) 1985, Intercomparison of Lageos orbit, polar motion and station coordinate solutions from two independent software systems, by Dow J M and Agrotis L G.
4. Dow J M and Agrotis L G, Polar motion and earth rotation series from Lageos. Pres. 26th Plenary Meeting of COSPAR, Symposium on Applications of Space Techniques for Geodesy and Geodynamics, Toulouse, July 1986.
5. Dow J M and Münch R E 1986, Precise orbit determination at ESOC: Experience, results and implications for future ESA missions, Proc. Second International Symposium on Spacecraft Flight Dynamics, Darmstadt, October 1986.
6. Hedin A E et al 1977, A global thermospheric model based on mass spectrometer and incoherent scatter data (MSIS), Journal of Geophys. Res., Vol. 82, No. 15, June 1977.
7. OAD-WP-316 (ESOC) 1986, Reduction of radial orbit error and generation of regional mean sea surfaces from analysis of SEASAT altimeter cross-overs, by Lecohier G, Dow J, Agrotis L G.
8. Lerch F J, March J G, Klosko S M and Williams R G, Gravity model improvement from SEASAT, J. Geophys. Res., 87, 3281-96, 1982.
9. Melbourne W (ed.) 1983, Merit standards, USNO Circular 167.
10. ESA Report CR(P) 2157 1985, Study of ionospheric and tropospheric models, by Rawer K and Bilitza D.
11. ESA/ESOC Contract 5227/82/D/IM(SC) 1983, Precise Orbit Determination for ERS-1, by Wakker K F, Ambrosius B A C and Aardoom L.
12. ESA/ESOC Contract 6140/84/D/IM 1986, Precise orbit computation, gravity model adjustment and altimeter data processing for the ERS-1 altimetry mission, by Wakker K F, Ambrosius B A C, Zandbergen and van Geldorp G.